

Glide Mechanisms for Bundle- and Plate-like Structures

R. Glüge

In this article, the slip mechanisms card deck glide and pencil glide are recaptured. These mechanisms are useful simplifications when several slip systems in crystals, bundle- or plate-like structures share a common shear plane \mathbf{n} or a common shear direction \mathbf{d} . It is pointed out that a third glide mechanism for slip systems with a common plane of shear $\mathbf{k} = \mathbf{d} \times \mathbf{n}$ exists. For this second pencil glide mechanism, its properties are examined, a flow rule is derived, and the push-forward of \mathbf{k} in case of large elastic strains is discussed. It turns out that the second pencil glide mechanism leads to a plane strain Prandtl-Reuss-like flow rule. Thus, unlike the pencil and the card glide mechanism, there is no accompanying lattice spin.

1 Introduction

Notation Throughout the work, a direct tensor notation is preferred. Vectors are symbolized by lowercase bold letters $\mathbf{v} = v_i \mathbf{e}_i$, second-order tensors by uppercase bold letters $\mathbf{T} = T_{ij} \mathbf{e}_i \otimes \mathbf{e}_j$, where \mathbf{e}_i with $i = \{1, 2, 3\}$ denotes the base vector of an orthonormal basis. The second order identity tensor is denoted by \mathbf{I} . The dyadic product is defined as $(\mathbf{a} \otimes \mathbf{b}) \cdot \mathbf{c} = (\mathbf{b} \cdot \mathbf{c})\mathbf{a}$. A dot represents a contraction. If more than one contraction is carried out, the number of dots corresponds to the number of vector pairs that are contracted, thus $\mathbf{a} \otimes \mathbf{b} \otimes \mathbf{c} \cdot \cdot \mathbf{d} \otimes \mathbf{e} = (\mathbf{b} \cdot \mathbf{d})(\mathbf{c} \cdot \mathbf{e})\mathbf{a}$, $\alpha = \mathbf{A} \cdot \cdot \mathbf{B}$. When only one contraction is carried out, the dot is frequently omitted, e.g. $\mathbf{A} = \mathbf{BC}$. The Euklidean norm of a vector and its counterpart for a second-order tensor, the Frobenius norm, are conveniently written as $|\mathbf{a}| = \sqrt{\mathbf{a} \cdot \mathbf{a}}$ and $\|\mathbf{A}\| = \sqrt{\mathbf{A} \cdot \cdot \mathbf{A}}$. The transpose of a second order tensor \mathbf{A} is denoted by \mathbf{A}^T , and defined through $\mathbf{A}\mathbf{a} = \mathbf{a}\mathbf{A}^T$ for all vectors \mathbf{a} .

Plastic Deformations of Single Crystals In 1934, Orowan (1934), Polanyi (1934) and Taylor (1934) found that the plastic deformation of most crystalline solids is realized by the movement of linear lattice imperfections, denominated as edge dislocations. On the crystal scale, the effect of collective dislocation movement manifests as crystallographic slip or glide, by the slipping of crystallographic planes parallel to each other. The direction of dislocation movement, which coincides for edge dislocations with the slip direction, is given by the dislocation Burgers vector. The latter is perpendicular to the edge dislocation. By this, the slip direction and the edge direction constitute a slip system: The edge direction of the dislocation spans together with the slip direction \mathbf{d} the shear plane \mathbf{n} . Both \mathbf{d} and \mathbf{n} need to be normalized, i.e. $|\mathbf{d}| = |\mathbf{n}| = 1$. This leads to the definition of the slip system tensor

$$\mathbf{M} = \mathbf{d} \otimes \mathbf{n}, \quad (1)$$

which is a crucial geometric information for the modelling of crystal plasticity. It can be used to calculate the shear stress acting inside the shear plane in direction of \mathbf{d} by projecting the stress vector

$$\mathbf{t} = \mathbf{T} \cdot \mathbf{n} \quad (2)$$

with the Cauchy stresses \mathbf{T} into the shear direction \mathbf{d} , i.e.

$$\tau = \mathbf{t} \cdot \mathbf{d} = \mathbf{T} \cdot \cdot \mathbf{M}. \quad (3)$$

If the slip system activity depends only on the resolved shear stress τ , one speaks about the Schmid law (Schmid, 1924; Georjieff and Schmid, 1926; Boas and Schmid, 1933). This simplification works well in many crystals, but is only a poor approximation for BCC crystals (Stein et al., 1973; Seeger, 2001).

In the commonly used multiplicative crystal plasticity framework, the deformation gradient is decomposed into an elastic and a plastic part,

$$\mathbf{F} = \mathbf{F}_e \mathbf{F}_p. \quad (4)$$

Mostly, the stresses \mathbf{T} are only a function of \mathbf{F}_e . With the product rule, the velocity gradient is then given by

$$\mathbf{L} = \dot{\mathbf{F}}\mathbf{F}^{-1} = \dot{\mathbf{F}}_e\mathbf{F}_e^{-1} + \mathbf{F}_e\dot{\mathbf{F}}_p\mathbf{F}_p^{-1}\mathbf{F}_e^{-1}, \quad (5)$$

$$\mathbf{L} = \mathbf{L}_e + \mathbf{L}_p, \quad \mathbf{L}_e = \dot{\mathbf{F}}_e\mathbf{F}_e^{-1}, \quad \mathbf{L}_p = \mathbf{F}_e\mathbf{L}_{p0}\mathbf{F}_e^{-1}, \quad (6)$$

where the abbreviation $\mathbf{L}_{p0} = \dot{\mathbf{F}}_p\mathbf{F}_p^{-1}$ is introduced. The rate of plastic deformation corresponds to the superposition of the slip rates of the active slip systems,

$$\mathbf{L}_{p0} = \sum_{i=1}^n \dot{\gamma}_i \mathbf{M}_{0i}. \quad (7)$$

Here, n denotes the number of active slip systems, $\mathbf{M}_{0i} = \mathbf{d}_{0i} \otimes \mathbf{n}_{0i}$, and \mathbf{d}_{0i} and \mathbf{n}_{0i} are the i^{th} normalized slip system vectors in an undeformed reference lattice. To relate the constant reference lattice to the stress state, one has to map \mathbf{d}_{0i} and \mathbf{n}_{0i} to the current placement. With the interpretation of \mathbf{d}_{0i} as a tangent vector and \mathbf{n}_{0i} as a gradient vector (see, e.g., Bertram (2008)), this mapping is given by

$$\mathbf{d}_i = \frac{\tilde{\mathbf{d}}_i}{|\tilde{\mathbf{d}}_i|}, \quad \tilde{\mathbf{d}}_i = \mathbf{F}_e \mathbf{d}_{0i}, \quad (8)$$

$$\mathbf{n}_i = \frac{\tilde{\mathbf{n}}_i}{|\tilde{\mathbf{n}}_i|}, \quad \tilde{\mathbf{n}}_i = \mathbf{F}_e^{-T} \mathbf{n}_{0i} = \mathbf{n}_{0i} \mathbf{F}_e^{-1}. \quad (9)$$

By this, $\tilde{\mathbf{d}}_i \cdot \tilde{\mathbf{n}}_i = 0$ holds. However, $\tilde{\mathbf{d}}_i$ and $\tilde{\mathbf{n}}_i$ are in general not of unit length, and require a normalization, which may be dropped only if the elastic strains are small. The initial values of \mathbf{F}_e and \mathbf{F}_p are given by relating the reference lattice to the initial placement. In the initial placement, one knows the orientation of the vectors \mathbf{d}_i , \mathbf{n}_i . With the constant reference lattice \mathbf{d}_{0i} , \mathbf{n}_{0i} , one can determine up to a lattice symmetry transformation the initial \mathbf{F}_e by eq. (9). \mathbf{L}_p is given by eqs. (6) to (9),

$$\mathbf{L}_p = \mathbf{F}_e \left(\sum_{i=1}^n (\dot{\gamma}_i \mathbf{d}_{0i} \otimes \mathbf{n}_{0i}) \right) \mathbf{F}_e^{-1} = \sum_{i=1}^n \dot{\gamma}_i \tilde{\mathbf{d}}_i \otimes \tilde{\mathbf{n}}_i. \quad (10)$$

Elasto-plasticity is considered to be integrable only by implicit time stepping schemes, since it is impossible to satisfy the consistency condition in ideal elastoplasticity by an explicit scheme. The consistency condition ensures that during plastic deformation the stress state remains on the yield surface. One can choose whether the evolution of \mathbf{F}_e or \mathbf{F}_p should be tracked, and obtain the other one from the multiplicative split,

$$\dot{\mathbf{F}}_e \mathbf{F}_e^{-1} = \mathbf{L} - \mathbf{L}_p, \quad \mathbf{F}_p = \mathbf{F}_e^{-1} \mathbf{F} \quad (11)$$

$$\dot{\mathbf{F}}_p \mathbf{F}_p^{-1} = \mathbf{L}_{p0}, \quad \mathbf{F}_e = \mathbf{F} \mathbf{F}_p^{-1}. \quad (12)$$

In the numerical time integration, both variants have their advantages. In monotonic processes, one may expect \mathbf{F}_e to saturate, allowing for larger time steps. But, since \mathbf{F}_e lives partially in the current placement, one has to integrate the rigid body spin, for which preferably an exact update algorithm is constructed (see, e.g., Chatti et al. (2001)). This is not necessary if \mathbf{F}_p is integrated (see, e.g., Krawietz (2001)).

Due to the orthogonality of the pairs $(\mathbf{d}_i, \mathbf{n}_i)$ and $(\mathbf{d}_{0i}, \mathbf{n}_{0i})$, the tensors \mathbf{M}_i and \mathbf{M}_{0i} and hence \mathbf{L} and \mathbf{L}_{p0} are deviatoric, which reflects the volume preservation under a shear deformation. A decomposition of \mathbf{L}_{p0} into its symmetric and antisymmetric part

$$\mathbf{D}_{p0} = \text{sym}(\mathbf{L}_{p0}) = \frac{1}{2}(\mathbf{L}_{p0} + \mathbf{L}_{p0}^T) \quad (13)$$

$$\mathbf{W}_{p0} = \text{skw}(\mathbf{L}_{p0}) = \frac{1}{2}(\mathbf{L}_{p0} - \mathbf{L}_{p0}^T) \quad (14)$$

is physically meaningful, since \mathbf{D}_{p0} is interpretable as the rate of plastic deformation, while \mathbf{W}_{p0} represents the lattice spin due to crystallographic slip. To realize an arbitrary isochoric deformation rate \mathbf{D}_{p0} , which has 5 independent components, at least 5 linearly independent symmetric contributions $\text{sym}(\mathbf{M}_{0i})$ are required. Mostly,

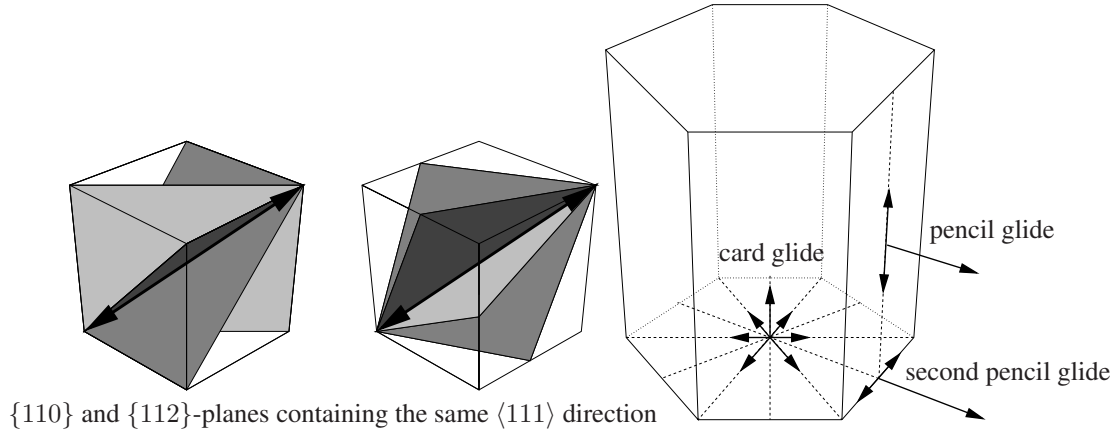


Figure 1: Left: $\langle 111 \rangle \{110\}$ and $\langle 111 \rangle \{112\}$ slip systems in a cubic lattice, sharing a common slip direction. Right: Possible glide mechanisms in a hexagonal lattice. The $\langle \bar{1}2\bar{1}0 \rangle \{0001\}$ slip systems have a common shear plane (card glide mechanism), the $\langle 0001 \rangle \{10\bar{1}0\}$ slip systems have a common slip direction (pencil glide) and the $\langle \bar{1}2\bar{1}0 \rangle \{10\bar{1}0\}$ slip systems share a common plane of shear (second pencil glide).

more than 5 linearly independent slip system tensors are available, which leaves the combination of slip rates accommodating the plastic strain undetermined, in the first place. To identify the active set of slip systems, different methods have been proposed, summarized by van Houtte (1988); Kocks (1998); Schurig (2006). Mostly, the slip system activity is uniquely related to the stress state by employing a rate-dependent rather than an ideal plastic behaviour in conjunction with the Schmid law. This is mostly done by Hutchinsons (Hutchinson, 1976) celebrated flow rule

$$\dot{\gamma}_i = \dot{\gamma}_0 \text{sgn}(\tau_i) \left| \frac{\tau_i}{\tau_{\text{crit}}} \right|^n, \quad (15)$$

with the strain rate sensitivity n , the critical shear stress τ_{crit} , and a reference shear rate $\dot{\gamma}_0$. The two latter parameters are redundant.

2 Slip Mechanisms with Constant Shear Direction or Constant Shear Plane Normal

In some materials, various slip directions are aligned parallel to a common shear plane, or a specific slip direction lies inside of several possible shear planes. Such characteristics can be found in bundle-structured (common slip direction) or in plate-structured (common shear plane) materials (Krawietz, 1981). Examples are the hexagonal close packed (HCP) crystal lattice, semi-crystalline polymers and the body-centered cubic (BCC) lattice. Although the BCC lattice does not display a bundle- or a plate-like structure, it contains a slip direction with a large number of corresponding slip plane normals. These slip systems are $\langle 111 \rangle \{110\}$ (3 planes per common slip direction), $\langle 111 \rangle \{112\}$ (3 planes per common slip direction) and $\langle 111 \rangle \{123\}$ (6 planes per common slip direction). Assuming that all these slip systems are potentially active under similar conditions, it may be convenient to replace the collective of slip systems by a slip mechanism with a continuously adjustable slip plane. We can thus drop the indexing of the individual slip systems. In case of a common slip direction, one speaks about the pencil glide mechanism (Taylor and Elam, 1926), while a set of slip systems having a common shear plane may be approximated by the card deck glide mechanism.

2.1 Card Deck Glide

In case of card deck glide, the shear plane normal is kept fixed, and \mathbf{d} is determined such that one considers the most critical out of the infinitely many slip systems. If the Schmid law is presumed, one may obtain \mathbf{d} by projecting the traction vector $\mathbf{t} = \mathbf{T} \cdot \mathbf{n}$ into the plane \mathbf{n} ,

$$\hat{\mathbf{d}} = (\mathbf{T} \cdot \mathbf{n}) \cdot (\mathbf{I} - \mathbf{n} \otimes \mathbf{n}). \quad (16)$$

The norm of $\hat{\mathbf{d}}$ gives the resolved shear stress, which is needed anyway for the normalization of $\hat{\mathbf{d}}$

$$\tau = |\hat{\mathbf{d}}|, \quad \mathbf{d} = \hat{\mathbf{d}}/\tau. \quad (17)$$

Then L_p is given by

$$L_p = \dot{\gamma}(\tau) \mathbf{d} \otimes \mathbf{n}. \quad (18)$$

Only in case that \mathbf{n} is an eigenvector of \mathbf{T} , the slip direction is evaluated to $\hat{\mathbf{d}} = \mathbf{0}$. Then, the Schmid stress results to be zero, \mathbf{d} is undefined, and no card glide is observed. Otherwise, the slip direction is uniquely determined by eq. (16).

2.2 Pencil Glide

In case of pencil glide, the normalized shear direction is kept fixed, and \mathbf{n} is determined such that one considers the most critical out of the infinitely many slip system. The slip system with orientation \mathbf{n} has the resolved shear stress

$$\tau(\mathbf{n}) = \mathbf{d} \cdot \mathbf{T} \cdot \mathbf{n} = (\mathbf{d} \cdot \mathbf{T} \cdot (\mathbf{I} - \mathbf{d} \otimes \mathbf{d})) \cdot \mathbf{n} = \hat{\mathbf{n}} \cdot \mathbf{n}, \quad (19)$$

$$\hat{\mathbf{n}} = (\mathbf{T} \cdot \mathbf{d}) \cdot (\mathbf{I} - \mathbf{d} \otimes \mathbf{d}). \quad (20)$$

As \mathbf{d} and consequently $\hat{\mathbf{n}}$ is fixed, we maximize this scalar product by aligning \mathbf{n} parallel to $\hat{\mathbf{n}}$. The resulting shear stress is then

$$\tau = |\hat{\mathbf{n}}|. \quad (21)$$

Again, the slip plane normal is uniquely determined if \mathbf{d} is not an eigenvector of \mathbf{T} .

2.3 Example Application

In case of only one slip mechanism and a constant stress state, the ODE for \mathbf{F}_p (eq. 12₁) is met by

$$\mathbf{F}_p(t) = (\mathbf{I} + \gamma(t)\mathbf{M}_0)\mathbf{F}_p(0). \quad (22)$$

Then, only $\gamma(t)$ needs to be determined consistently. An example is the card glide mechanism in hexagonal lattices. In magnesium at room temperature, only basal glide in the systems $\langle 11\bar{2}0 \rangle \{0001\}$ may occur, which allows to reduce the overall slip system activity to only one card glide mechanism. But even if more than one glide mechanism needs to be considered, the system of nonlinear equations to be solved is simplified, since the unknown shear directions (card glide) and the unknown shear plane normals (pencil glide) are determined uniquely by the stress state (Krawietz, 2001).

Both mechanisms have proved to be useful approximations, see, e.g. Park et al. (1996); Raabe (1997); Cai et al. (2009); Glüge et al. (2010). One advantage of these approximations is that the number of slip systems is reduced, and the numerical time integration is simplified considerably. Then, the slip direction (card glide) or slip plane normal (pencil glide) may be assumed to be incrementwise constant.

3 Slip Mechanism with Constant Plane of Shear

Another possible slip system alignment of a set of slip systems is inside a common *plane of shear* \mathbf{k} , which is spanned by \mathbf{d} and \mathbf{n} , not to be confused with the *shear plane* \mathbf{n} . Such a slip mechanism may be found in bundle-structured materials. Here, it is referred to as the *second pencil glide* mechanism. For example, the prismatic slip systems in a hcp lattice given by $\langle \bar{1}2\bar{1}0 \rangle \{ \bar{1}010 \}$ have a common plane of shear $\mathbf{k} = \mathbf{d} \times \mathbf{n}$, namely the $\{0001\}$ plane (see Fig. 1). Another example is the transverse slip in semi-crystalline polymers, where polymeric chains glide along each other either parallel or transverse (G'Sell and Dahoun, 1994).

Suppose that, for a given stress state \mathbf{T} , a common plane of shear \mathbf{k} and a relation between the Schmid stress and the slip rate $\dot{\gamma}(\tau)$, the plastic deformation rate has to be determined. All potential slip and shear plane directions lie inside the plane \mathbf{k} . Therefore, a projection of \mathbf{d} or \mathbf{n} into the common plane of shear does not alter \mathbf{d} or \mathbf{n} at all, and we may expand the calculation of the Schmid stress according to

$$\tau = \mathbf{d} \cdot \mathbf{T} \cdot \mathbf{n} = \mathbf{d} \cdot \underbrace{\mathbf{P}_k \cdot \mathbf{T} \cdot \mathbf{P}_k}_{\mathbf{T}^*} \cdot \mathbf{n}, \quad (23)$$

with the projector

$$\mathbf{P}_{\mathbf{k}} = \mathbf{I} - \mathbf{k} \otimes \mathbf{k}. \quad (24)$$

Dealing with $\mathbf{T}^* = \mathbf{P}_{\mathbf{k}} \mathbf{T} \mathbf{P}_{\mathbf{k}}$ instead of \mathbf{T} allows a direct calculation of the maximum shear stresses acting inside the potential slip systems, since \mathbf{T}^* represents a plane stress state. With a zero eigenvalue $T_3^* = 0$ in the eigendirection of \mathbf{k} , the remaining eigenvalues T_1^* and T_2^* are the roots of a quadratic equation. After obtaining $T_{1,2}^*$ with the ordering $T_1^* > T_2^*$ and the normalized eigenvectors $\mathbf{t}_1, \mathbf{t}_2$, one is able to compute the maximum shear stress by

$$\tau_{\max} = \frac{1}{2}(T_1^* - T_2^*). \quad (25)$$

The planes of maximum shear stress are aligned 45° of the principal stress axes. The two slip systems with extremal positive resolved shear stresses are given by

$$\mathbf{M}_1 = \mathbf{v}_1 \otimes \mathbf{v}_2 \quad (26)$$

$$\mathbf{M}_2 = \mathbf{v}_2 \otimes \mathbf{v}_1 = \mathbf{M}_1^T \quad (27)$$

$$\mathbf{v}_1 = \frac{1}{\sqrt{2}}(\mathbf{t}_1 + \mathbf{t}_2) \quad (28)$$

$$\mathbf{v}_2 = \frac{1}{\sqrt{2}}(\mathbf{t}_1 - \mathbf{t}_2). \quad (29)$$

Due to the symmetry of \mathbf{T} , the maximum shear stress is encountered simultaneously in the two slip systems \mathbf{M}_1 and \mathbf{M}_2 . Using the projector representation

$$\mathbf{T}^* = T_1^* \mathbf{t}_1 \otimes \mathbf{t}_1 + T_2^* \mathbf{t}_2 \otimes \mathbf{t}_2, \quad (30)$$

one can review easily that

$$\tau_{\max} = \frac{1}{2}(T_1^* - T_2^*) = \mathbf{T}^* \cdot \cdot \mathbf{M}_1 = \mathbf{T}^* \cdot \cdot \mathbf{M}_2 = \tau_1 = \tau_2. \quad (31)$$

It is interesting to note that in the viscoplastic case, the plastic deformation rates are equal in both slip systems because of $\tau_1 = \tau_2$. Together with $\mathbf{M}_2 = \mathbf{M}_1^T$, it is to conclude that there is no plastic spin in the viscoplastic case. In case of ideal plasticity, the plastic spin is undetermined. If hardening is added, the $\dot{\gamma}_1$ and $\dot{\gamma}_2$ are related by the consistency condition. Presuming $\dot{\gamma} = \dot{\gamma}_1 = \dot{\gamma}_2$, one obtains

$$\mathbf{L}_p = \dot{\gamma}(\mathbf{M}_1 + \mathbf{M}_2) \quad (32)$$

$$= \dot{\gamma} \left(\frac{1}{2}(\mathbf{t}_1 + \mathbf{t}_2) \otimes (\mathbf{t}_1 - \mathbf{t}_2) + \frac{1}{2}(\mathbf{t}_1 - \mathbf{t}_2) \otimes (\mathbf{t}_1 + \mathbf{t}_2) \right) \quad (33)$$

$$= \dot{\gamma}(\mathbf{t}_1 \otimes \mathbf{t}_1 - \mathbf{t}_2 \otimes \mathbf{t}_2). \quad (34)$$

Therefore, the overall deformation rate results to be symmetric, coaxial to \mathbf{T}^* , and deviatoric. One notes that, since \mathbf{L}_p is symmetric, the second pencil glide mechanism does not induce a lattice spin, unlike the card glide and the pencil glide mechanism. Since \mathbf{L}_p is coaxial to \mathbf{T}^* , one may rewrite the second pencil glide mechanism similar to the Prandtl-Reuss relation, i.e. like

$$\mathbf{L}_p = \dot{\gamma} \mathbf{N}. \quad (35)$$

To determine the normalized flow direction $\mathbf{N} = \hat{\mathbf{N}} / \|\hat{\mathbf{N}}\|$, one has to project \mathbf{T} firstly to \mathbf{T}^* , and then take the deviatoric part only on the remaining two-dimensional eigenspace with nonzero eigenvalues. This is achieved by

$$\hat{\mathbf{N}} = \mathbf{T}^* - \frac{1}{2}(\mathbf{P}_{\mathbf{k}} \cdot \cdot \mathbf{T}^*) \mathbf{P}_{\mathbf{k}} \quad (36)$$

$$= T_1^* \mathbf{t}_1 \otimes \mathbf{t}_1 + T_2^* \mathbf{t}_2 \otimes \mathbf{t}_2 - \frac{1}{2}(T_1^* + T_2^*)(\mathbf{t}_1 \otimes \mathbf{t}_1 + \mathbf{t}_2 \otimes \mathbf{t}_2) \quad (37)$$

$$= \frac{1}{2}(T_1^* - T_2^*) \mathbf{t}_1 \otimes \mathbf{t}_1 + \frac{1}{2}(T_2^* - T_1^*) \mathbf{t}_2 \otimes \mathbf{t}_2, \quad (38)$$

which is seen easily by using the projector representation of \mathbf{T}^* and $\mathbf{P}_{\mathbf{k}} = \mathbf{t}_1 \otimes \mathbf{t}_1 + \mathbf{t}_2 \otimes \mathbf{t}_2$. Inserting $\mathbf{T}^* = \mathbf{P}_{\mathbf{k}} \mathbf{T} \mathbf{P}_{\mathbf{k}}$ into eq. (36) allows with $\mathbf{P}_{\mathbf{k}} \cdot \cdot \mathbf{P}_{\mathbf{k}} = \mathbf{P}_{\mathbf{k}}$ to summarize to

$$\hat{\mathbf{N}} = \mathbf{P}_{\mathbf{k}} \cdot \cdot \mathbf{T} \cdot \cdot \mathbf{P}_{\mathbf{k}} - \frac{1}{2}(\mathbf{P}_{\mathbf{k}} \cdot \cdot \mathbf{T}) \mathbf{P}_{\mathbf{k}}. \quad (39)$$

The difference $\hat{N}_1 - \hat{N}_2$ of the two nonzero eigenvalues $\hat{N}_1 = \frac{1}{2}(T_1^* - T_2^*)$ and $N_2 = \frac{1}{2}(T_2^* - T_1^*)$ results in

$$\hat{N}_1 - \hat{N}_2 = T_1^* - T_2^*. \quad (40)$$

Comparing with eq. (25) and taking into account that $\hat{N}_1 = -\hat{N}_2$, we can determine the maximum Schmid stress by

$$\tau_{\max} = \hat{N}_1 \quad (41)$$

which can be reduced with $\|\hat{\mathbf{N}}\| = \sqrt{2}\hat{N}_1$ to

$$\tau_{\max} = \frac{\|\hat{\mathbf{N}}\|}{\sqrt{2}}. \quad (42)$$

By noting that a normalization of $\hat{\mathbf{N}}$ gives the flow direction

$$\hat{\mathbf{N}}/\|\hat{\mathbf{N}}\| = \frac{1}{\sqrt{2}}(\mathbf{t}_1 \otimes \mathbf{t}_1 - \mathbf{t}_2 \otimes \mathbf{t}_2), \quad (43)$$

we are able to summarize the flow rule (eq. 34) as

$$\mathbf{L}_p = \dot{\gamma} \left(\frac{\|\hat{\mathbf{N}}\|}{\sqrt{2}} \right) \frac{\hat{\mathbf{N}}}{\|\hat{\mathbf{N}}\|}, \quad \hat{\mathbf{N}} = \mathbf{P}_k \mathbf{T} \mathbf{P}_k - \frac{1}{2}(\mathbf{P}_k \cdot \mathbf{T}) \mathbf{P}_k. \quad (44)$$

This reformulation has the advantage that it does not require an explicit determination of the eigenvalues and eigendirections.

4 Transformation of \mathbf{k}

Since a clear interpretation as tangent and gradient vectors for \mathbf{d} and \mathbf{n} is given, the treatment of the card glide and the pencil glide mechanism differs only slightly: Calculate $\mathbf{d} = \mathbf{F}_e \mathbf{d}_0 / |\mathbf{F}_e \mathbf{d}_0|$ or $\mathbf{n} = \mathbf{F}_e^{-T} \mathbf{n}_0 / |\mathbf{F}_e^{-T} \mathbf{n}_0|$ and apply the equations given in Section 2.1 or 2.2 to obtain τ , the missing slip system vector \mathbf{n} or \mathbf{d} , $\dot{\gamma}$, and finally \mathbf{L}_p . Then integrate

$$\dot{\mathbf{F}}_e \mathbf{F}_e^{-1} = \mathbf{L} - \mathbf{L}_p \quad (45)$$

or

$$\dot{\mathbf{F}}_p \mathbf{F}_p^{-1} = \mathbf{F}_e \mathbf{L}_p \mathbf{F}_e^{-1}. \quad (46)$$

In case of the second pencil glide mechanism, the question of how \mathbf{k}_0 should be transformed to \mathbf{k} arises. One can easily see that there exists no linear transformation similar to \mathbf{d} and \mathbf{n} that ensures $\mathbf{k} \cdot \mathbf{d} = 0$ and $\mathbf{k} \cdot \mathbf{n} = 0$ at the same time. Therefore, one might think of taking $\mathbf{k} = \mathbf{d} \times \mathbf{n}$ after obtaining \mathbf{d} and \mathbf{n} by eq. (9). This is as well problematic, since inside the common plane of shear \mathbf{k}_0 , any perpendicular pair $\mathbf{v}_{10}, \mathbf{v}_{20}$ constitutes a valid slip system. Hence one can take either $\mathbf{d}_0 = \mathbf{v}_{10}, \mathbf{n}_0 = \mathbf{v}_{20}$ or $\mathbf{d}_0 = \mathbf{v}_{20}, \mathbf{n}_0 = \mathbf{v}_{10}$, which results up to the sense of direction in the same \mathbf{k}_0 , but in distinct \mathbf{k} .

As it is the case for \mathbf{d} and \mathbf{n} , one has to think about the physical interpretation of \mathbf{k}_0 to determine whether \mathbf{k}_0 should be transformed as a gradient or a tangent vector.

Transformation as a Gradient Vector $\mathbf{k} = \mathbf{F}_e^{-T} \mathbf{k}_0 / |\mathbf{F}_e^{-T} \mathbf{k}_0|$: The common plane of shear is given by the deformed reference cross-section of the bundle. This interpretation is reasonable if the slip mechanism involves discrete points on the bundles, as it is the case for dislocation movement. The lattice sites that are passed by the dislocation are attached to the lattice.

Transformation as a Tangent Vector $\mathbf{k} = \mathbf{F}_e \mathbf{k}_0 / |\mathbf{F}_e \mathbf{k}_0|$: The common plane of shear is given by the cross-section of the deformed bundle. This interpretation is reasonable if the slip mechanism does not depend on discrete points on the bundles, i.e., if the bundles can be regarded as continuous and, with reference to the deformation

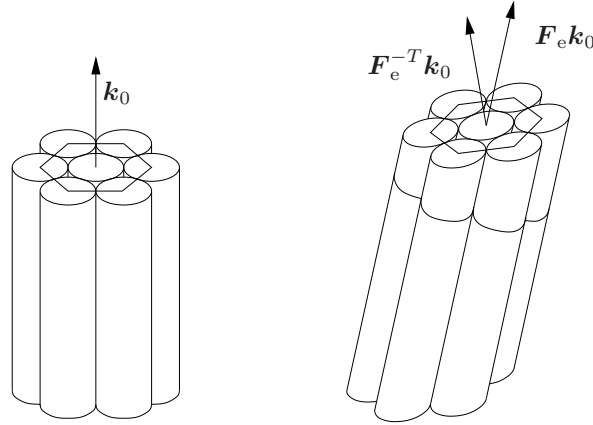


Figure 2: Left: Undeformed bundle, with \mathbf{k}_0 . Right: Deformed bundle with $\mathbf{F}_e \mathbf{k}_0$ being the cross-section normal of the deformed bundle and $\mathbf{F}_e^{-T} \mathbf{k}_0$ the normal vector of the deformed reference cross-section.

mechanism, free of distinguished points along the bundle axis.

Therefore, depending on the modeling scale, one will chose $\mathbf{k} = \mathbf{F}_e^{-T} \mathbf{k}_0$ if the underlying deformation mechanism can be linked to the atomic scale, and $\mathbf{k} = \mathbf{F}_e \mathbf{k}_0$ if the bundles are regarded as continuous and without discrete connections among them. After obtaining \mathbf{k} , the treatment given in Section 3 can be applied, which yields the plastic velocity gradient \mathbf{L}_p , and therefore an evolution equation for \mathbf{F}_e or \mathbf{F}_p (eqs. 45 and 46).

5 Summary

Besides the well known card and pencil glide mechanisms, a third glide mechanism for slip systems that are aligned inside a common plane of shear exists. This second pencil glide mechanism may prove to be useful in bundle-like structures. Possible applications are the transverse slipping of chains in polymeric crystals and the prismatic slip systems in hexagonal lattices. Unlike the card and pencil glide mechanisms, the second pencil glide does not induce a lattice spin. Instead, inside the common plane of shear, the plastic deformation behaves isotropically, which allows to obtain a flow rule similar to the Prandtl-Reuss equation. In case of non-negligible elastic deformations, the plane of shear normal \mathbf{k}_0 is transformed as a gradient vector if the underlying deformation mechanism is linked to discrete connections between the bundles, and like a tangent vector if no such distinguished connections prevail.

Acknowledgment: For helpful advice and discussions, I would like to express my gratitude to my colleague Jan Kalisch and the unknown reviewer.

References

- Bertram, A.: *Elasticity and Plasticity of Large Deformations - an Introduction, Second Edition*. Springer Verlag, Berlin (2008).
- Boas, W.; Schmid, E.: Zur Fließbedingung von Kristallen. *Zeitschrift für Physik A*, 86, 11-12, (1933), 828–830.
- Cai, S.; Daymond, M.; Khan, A.; Holt, R.; Oliver, E.: Elastic and plastic properties of β -Zr at room temperature. *Journal of Nuclear Materials*, 393, 1, (2009), 67–76.
- Chatti, S.; Dogui, A.; Dubujet, P.; Sidoroff, F.: An objective incremental formulation for the solution of anisotropic elastoplastic problems at finite strain. *Communications in Numerical Methods in Engineering*, 17, 12, (2001), 845–862.
- Georgieff, M.; Schmid, E.: Über die Festigkeit und Plastizität von Wismutkristallen. *Zeitschrift für Physik*, 36, 9-10, (1926), 759–774.
- Glüge, R.; Bertram, A.; Böhlke, T.; Specht, E.: A pseudoelastic model for mechanical twinning on the microscale. *Zeitschrift für Angewandte Mathematik und Mechanik*, 90, 7-8, (2010), 565–594.

- G'Sell, C.; Dahoun, A.: Evolution of microstructure in semi-crystalline polymers under large plastic deformation. *Materials Science and Engineering A*, 175, (1994), 183–199.
- Hutchinson, J.: Bounds and self-consistent estimates for creep of polycrystalline materials. *Proceedings of the Royal Society of London. Series A: Mathematical, Physical and Engineering Sciences*, 348, (1976), 101–127.
- Kocks, U.: *Texture and Anisotropy*, chap. 8: Kinematics and Kinetics of Plasticity, pages 327–389. Cambridge University Press (1998).
- Krawietz, A.: Passivität, Konvexität und Normalität bei elastisch-plastischem Material. *Ingenieur-Archiv*, 51, (1981), 257–274.
- Krawietz, A.: Efficient integration in the plasticity of crystals with pencil glide and deck glide. *Technische Mechanik*, 21, 4, (2001), 243–250.
- Orowan, E.: Zur Kristallplastizität: iii. Über den Mechanismus des Gleitvorganges. *Zeitschrift für Physik*, 89, (1934), 634–659.
- Park, Y.; Raabe, D.; Yim, T.: Cold rolling textures of FeNi soft magnetic alloys. *Scripta Materialia*, 35, 11, (1996), 1277–1283.
- Polanyi, M.: Über eine Art Gitterstörung, die einen Kristall plastisch machen könnte. *Zeitschrift für Physik*, 89, (1934), 660–664.
- Raabe, D.: Texture and microstructure evolution during cold rolling of a strip cast and of a hot rolled austenitic stainless steel. *Acta Materialia*, 45, 3, (1997), 1137–1151.
- Schmid, E.: Bemerkungen über die plastische Deformation von Kristallen. *Zeitschrift für Physik*, 22, 1, (1924), 328–333.
- Schurig, M.: The Vertex Effect in Polycrystalline Materials, Ph.-D.-Thesis. <http://diglib.uni-magdeburg.de/Dissertationen/2006/micschurig.pdf> (2006).
- Seeger, A.: Why anomalous slip in body-centred cubic metals? *Materials Science and Engineering A*, 319–321, (2001), 254–260.
- Stein, D.; Wang Chen, C.; Ayres, R.: *The Inhomogeneity of Plastic Deformation*, chap. The Anisotropy of Yielding in Single Crystals, pages 55–112. American Society for Metals (1973).
- Taylor, G.: The mechanism of plastic deformation of crystals. Part I. theoretical. *Proceedings of the Royal Society of London. Series A*, 145, (1934), 362–387.
- Taylor, G.; Elam, C.: The Distortion of Iron Crystals. *Proceedings of the Royal Society of London. Series A: Mathematical, Physical and Engineering Sciences*, 112, 1, (1926), 337–361.
- van Houtte, P.: A comprehensive mathematical formulation of an extended Taylor-Bishop-Hill model of featuring relaxed constraints, the Renouard-Wintenberger theory and a strain rate sensitivity model. *Textures and Microstructures*, 8-9, (1988), 313–350.

Address: Universitätsplatz 2, D-39106 Magdeburg
 email: gluege@ovgu.de